Vivaldi antennas: a historical review and current state of art

Anindita Bhattacharjee[1], Abhirup Bhawal[1], Anirban Karmakar[1] (iD),
Anuradha Saha[2] and Diptendu Bhattacharya[3]

[1]Electronics & Communication Engineering Department, Tripura University (A Central University), Tripura, India;
[2]Netaji Subhash Engineering College, Garia, Kolkata, India and [3]CSE Department, NIT, Agartala, India

CAMBRIDGE
UNIVERSITY PRESS

Abstract

The progressions in the field of wireless technology can be highly attributed to the development of antennas, which can access high data rates, provide significant gain and uniform radiation characteristics. One such antenna called the Vivaldi antenna has attracted the utmost attention of the researchers owing to its high gain, wide bandwidth, low cross-polarization, and stable radiation characteristics. Over the years, different procedures have been proposed by several researchers to improve the performance of the Vivaldi antennas. Some of these different approaches are feeding mechanisms, integration of slots, dielectric substrate selection, and radiator shape. Correspondingly, the performance of a Vivaldi antenna can be increased by including dielectric lens, parasitic patch in between two radiators, corrugations, as well as metamaterials. This paper gives a systematic identification, location, and analysis of a large number of performance enhancement methods of Vivaldi antenna design depicting their concepts, advantages, drawbacks, and applications. The principal emphasis of this article is to offer an outline of the developments in the design of Vivaldi antennas over the last few years, where the most important offerings, mostly from IEEE publications, have been emphasized. This review work aims to reveal a promising path to antenna researchers for its advancement using Vivaldi antennas.

Introduction

As the demand for broadcast and wireless communication technologies is increasing day by day, the necessity of planning a new type of antenna with features like broader impedance bandwidth and highly directive radiation pattern has increased. Directional antennas are mostly used in applications to enhance the wireless systems' capacity and to reduce the effect of co-channel interference and multipath effects. Wideband antennas are used in different applications like satellite communication, RADAR, microwave imaging systems, remote-sensing systems, GPR detection, and medical applications. On the other hand, wideband antennas are also found useful in broadband communication to replace the need for multiple antennas for diversified applications due to its features like less complexity, lower power consumption, and a more compact footprint. Vivaldi antennas has been found as is one of the suitable candidates for a broadband directional communication system.

Gibson [1], in the year 1979, first introduced the Vivaldi Antenna, which belongs to the class of end-fire traveling antennas. The Vivaldi antenna offers the feature of a slot line in which edge separation of the slot line extends higher than $X/2$, where X is the length of the parameter. The non-resonant traveling wave mechanism of radiation of a Vivaldi antenna is produced by a higher-order Hankel function [1]. The main requirement for the gain of the Vivaldi antenna is that the bounded wave phase velocity should be equal to or exceed the surrounding medium, which needs a continuous phase leading compensation of the traveling wave structure. The Vivaldi antenna provides end-fire radiation with a beam width approximately the same for E- and H-planes. For achieving constant beam width, the shape of the antenna is ultimately expressed in terms of the wavelength, which is a dimensionless quantity. The video receiver module in [1] is designed using a Vivaldi antenna and an integrated broadband video detector unit. The designed curve is in the form used in Fig. 1 with $Y = \pm AePX$, where Y represents the distance of half separation and X means the length parameter. The magnification factor P determines the bandwidth. The radiating conductor slot plane of Vivaldi antenna is designed on an alumina substrate using the following equation [1].
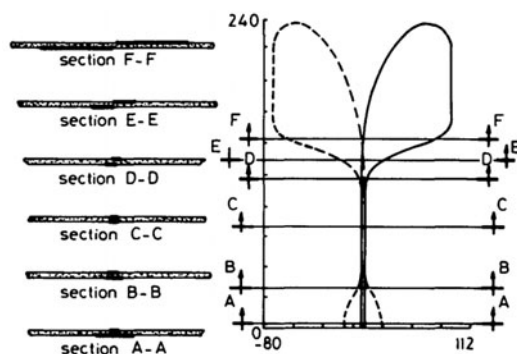
$$Y = \pm 0.125 \ \exp{(0.052X)}, \tag{1}$$

where X and Y represent dimensions to a new origin at the radiator feed.

Vivaldi antenna belongs to a class of a periodic, gradually curved slow leaky end-fire traveling antenna. The different portions of the antenna radiate different frequencies, but the size
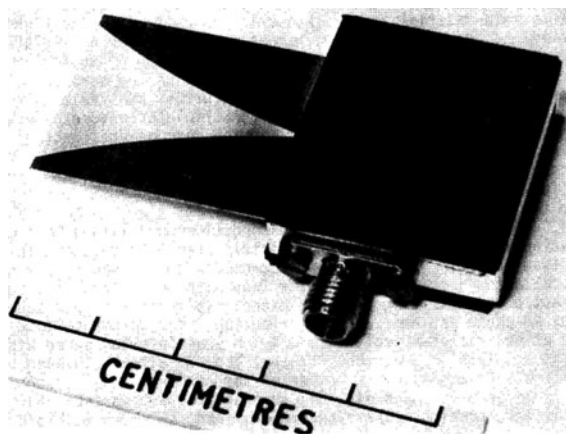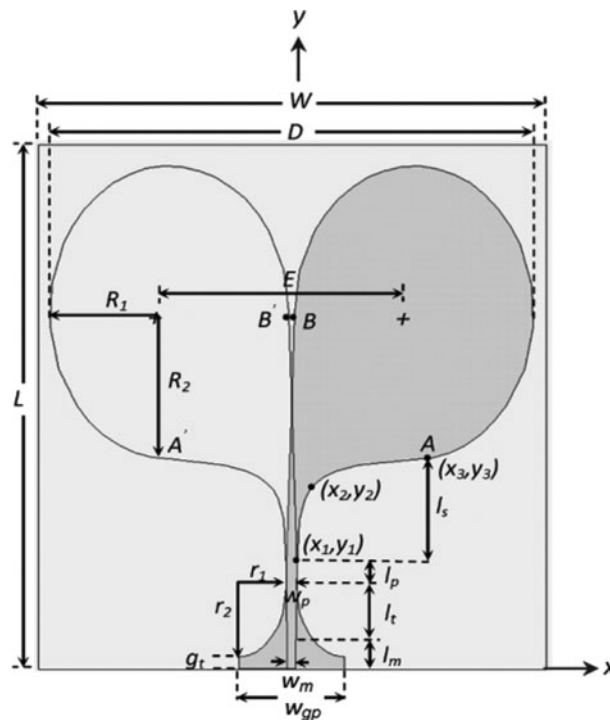
Fig. 1. 8–40 GHz Video Receiver Module shows a video receiver module operates in the range of 8–40 GHz [1].

Fig. 2. Transition from microstrip to symmetric slot line and Vivaldi antenna [3].

Fig. 3. Schematic of an antipodal TSA using balun transformer as feed with $W = D + 8$, $D = 2R_1 + E$, $L = 2R_2 + l_s + l_p + l_t + l_m + 4$, $R_1 = 68$, $R_2 = 1.3R_1$, $E = 2R_1 + 2$, $r_1 = 43.2$, $r_2 = 27$, $(x_1, y_1) = (2.975, 60)$, $(x_2, y_2) = (12, 110)$, $(x_3, y_3) = (69, 126.6)$, $l_s = 66.6$, $l_p = 10$, $l_t = 42.5$, $l_m = 7.5$, $w_p = 5.95$, $w_m = 4.65$, $w_{gp} = 60$, $g_t = 8$ (all parameters are in mm) [8].

of the radiating part becomes constant with wavelength. It has infinite bandwidth [2], but due to transition in the feeding section, i.e. transition from the transmission line to slot line the bandwidth is reduced. Another property of a Vivaldi antenna is constant beam width with respect to frequency, but it is also dependent on the proper designing of the antenna. Two major concerns for designing a Vivaldi antenna operating in the microwave range are the transition in the feeding structure and the dimension and shape of the antenna to attain a concentrated beam width. The Vivaldi antenna is mostly fed by using a balanced slot line. Some researchers use substrates with high dielectric constants and a small hole to connect the conductor. The process of tapered transition from microstrip to symmetric slot line and Vivaldi antenna with the change from microstrip to symmetric double-sided slot line is shown in Fig. 2.

The transition in the feeding structure is done by tapering the microstrip line. Due to the transition in the feeding structure, the antenna produces low return loss over an extensive frequency range. The antenna also provides restrained beam width due to tapering of the slot line in the exponential form. To reduce the sidelobe gain, the end of the antenna should be curved. There are three areas namely feed area, transit area, and radiation area found in Vivaldi antenna. For electromagnetic coupling, the feed area is responsible. A modified structure of the antenna was developed by Gazit [3] to overcome the drawbacks of the Exponential Tapered Slot Antenna (ETSA) [1], which was

known as the antipodal Vivaldi antenna (AVA). The bandwidth of ETSA can be enhanced by using the AVA because of its feeding technique, e.g. microstrip line-to-double-sided parallel stripline. Another type of Vivaldi antenna was introduced by Langley *et al.* [4] to overcome the drawbacks of AVA. The antenna is known as balanced AVA (BAVA). This antenna has the widest bandwidth, but the main disadvantages are its high cost and intricate design. They have been extensively used in different fields such as satellite communications, radars, microwave imaging systems, remote-sensing systems, and medical field for detecting tumor cell and cancer cell and telescopes.

Feeding mechanism of Vivaldi antennas

In Vivaldi antennas, the power transfer between a source and antenna is done through a feed line. In general, the characteristic impedance of a transmission line is $50\,\Omega$. By maximum power transfer theorem, the Vivaldi antenna should be fed at a point where input impedance is $50\,\Omega$ for full input power. There are various feeding techniques for the Vivaldi antenna to match this condition. In [5], a tapered microstrip feeding line with a fixed port width of 1.5 mm is adopted for perfect impedance matching. A feed transition structure is utilized to feed AVA, which is designed with a broad working band and low insertion loss in [6]. This transition from broadside parallel stripline to coplanar waveguide (CPW) makes this AVA cooperate reasonably with integrated microwave circuits. A compact tapered bending microstrip line feed is used in [7] to provide wide impedance matching. The feed line consists of two metallic bending lines on both sides of the substrate. The feed design for the antipodal TSA found in [8] comprises sections, as shown in Fig. 3,
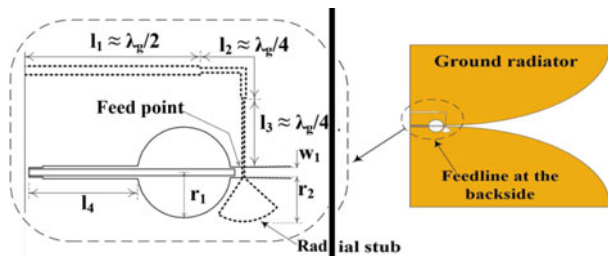
Fig. 4. Two-stage quarter-wave balun with $l_1 = 26.7$ mm, $l_2 = l_3 = 11.7$ mm, $l_4 = 17.2$ mm, $w_1 = 1.65$ mm, $r_1 = 7.1$ mm, $r_2 = 6.7$ mm. (a) Detailed geometry of balun. (b) Front/back view of the antenna [20].

consisting of an elliptically contoured ground plane, a microstrip line, and a parallel plate, thus forming the balun transformer for broadband matching. A similar approach is used in [9] with a microstrip-to-slot line transition balun exciting the Vivaldi antenna for a broadband impedance matching.

An exponential tapered microstrip line is implemented in [10] for excitation of a nature fern inspired fractal leaf structured antenna. A transition with an exponential form factor between the feed line and the radiator is introduced here which affects the impedance bandwidth. In [11], a microstrip feed, which is centered with respect to the exponential flares of the corrugated Vivaldi antenna, is utilized with a radial open stub at the end to increase the input impedance bandwidth. A conventional AVA is fed through a microstrip line in [12] with a width of 1.14 mm to match with the 50 Ω coaxial line to achieve optimum bandwidth for detection of a void inside concrete structures. The structure of a compact Vivaldi antenna with a simple coaxial feed for wideband application is seen in [13]. In [14], a two-stage coupled bandpass filter is implemented in the feed and terminated with a K-type connector, which is connected to two open shunt stubs, for low insertion loss, proper impedance matching, and sufficient bandwidth. In [15], a new stepped connection feed structure between slot line and tapered patches is adopted in a planar printed Vivaldi antenna. By using the stepped connection structure, the impedance matching is significantly improved, and wide bandwidth is achieved. A highly directed Vivaldi antenna structure is obtained in [16] where the radiator is fed by a tapered microstrip line and slot line for impedance transformation from 50 Ω to about 80 Ω. In [17], a microstrip line to a symmetric double-sided slot line formation is used, which makes the input impedance conveniently matched to 50 Ω within a broadband. In [18], the design of a three-port diversity antenna capable of producing three-directional radiation pattern for vehicular communications is presented. The proposed antenna consists of three uncorrelated Vivaldi antennas with three individual coaxial feeds developed on a single printed circuit board which offers ultra-wideband (UWB) characteristics with end-fire radiation pattern leading to high realized antenna gain. In [19], a conventional Vivaldi antenna is excited by a balun which consists of a T-junction power divider and two transition structures. The two transitions are a microstrip to CPW transition and a microstrip to coplanar stripline transition that are adopted to achieve wideband phase and magnitude balance resulting in wideband radiation performance. In [20], a two-stage quarter-wave balun structure is implemented at the feed point of two orthogonally crossed Vivaldi antennas to achieve UWB property as seen in Fig. 4.

In [21], a conventional Vivaldi antenna is fed by a balun consisting of two different forms of transition structures. The first transition is realized by connecting the microstrip line to the slot line through short-ended via and the second transition is achieved by introducing electromagnetic coupling between the slot line and the output microstrip line. With the adoption of the balun structure, the unbalanced signal to balanced signals transition is achieved, leading to wideband performance. The antenna structure proposed in [22] consists of two orthogonal Vivaldi antenna elements, and the mode of feeding adopts electromagnetic coupling from the microstrip line to slot line. The improved balun can avoid the intersection of transmission lines, reduce the size, and simplify the assembly. A novel compact end-fire AVA is proposed for UWB applications in [23]. A bending feed line structure and sinusoidal modulated Gaussian tapered slot are employed to make the antenna compact. In [24] a novel high gain circularly polarized (CP) antenna array for 5G applications is presented. The array element is an antipodal curvedly tapered slot antenna (ACTSA) producing CP field. The CP ACTSA fed by substrate-integrated waveguide is suitable to incorporate with substrates.
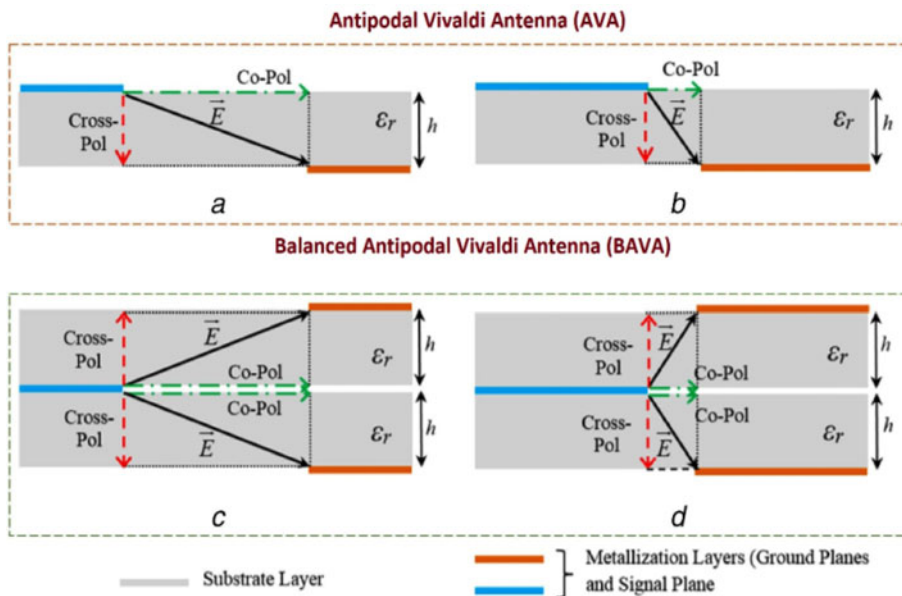
Balanced and unbalanced AVA

The BAVA as proposed by Langley *et al.* [4] incorporates an ultra-wide bandwidth transition and overcomes the poor polarization performance of the basic unbalanced antipodal form [3]. The structure of BAVA consists of three copper layers with the outer two copper layers acting as ground layers and the middle layer as a conductor. All copper layers are separated by substrates. As seen in Fig. 7, this structure equipoises the loading of dielectric material in between conductor and ground plane. Due to this balancing, changes in beam direction due to frequency, polarization, or orientation (called beam squint [25]) are highly reduced as can be seen from Fig. 5. In [26], the BAVA having an elongated substrate is loaded with slots resulting in increased end-fire performance and a higher front to back ratio. In [27], BAVA with transformation optics is used to enhance the gain, sidelobe level, and cross-polarization. Antenna gain and beam tilting can be refined by introducing a patch in between two flares of a BAVA, as seen in [28]. In [29], the beam squint can be lowered prominently by eliminating substrate in between two copper flares of the BAVA. Table 1 lists the performance comparison of BAVA design (Fig. 6).

Moreover, a compact BAVA with corrugation is observed in [29]. Figures 7(a) and 7(b) show the top and bottom views of the typical fabricated BAVA, respectively. This BAVA is designed by using corrugation, slots, and by removing substrate present in between two flares. Figure 7(c) shows that the modified BAVA minimizes beam squint. BAVA with improved return loss and bandwidth is demonstrated in [31]. A wideband BAVA is transformed to notch band BAVA in [30] by introducing a quarter wavelength spur line in the microstrip feed line. Four types of BAVA as conventional BAVA, BAVA with symmetric substrate cut-out (BAVA-SC), BAVA with asymmetric cut-out (BAVA-AC), and BAVA-AC with dual-scale slotted edges (BAVA-AC-DSE) are implemented here. An acceptable reduction in sidelobe levels can be seen in Fig. 7(d) by using BAVAAC-DSE.

## Vivaldi antenna for wideband applications

In February 2002, the Federal Communications Commission (FCC) assigned 3.1 GHz from 10.6 GHz to UWB spectrum for public use [32]. UWB is an alternative for narrowband technology. Since 2002, UWB technology has been recognized as one of the most indispensable and a foremost choice in wireless

Fig. 5. Schematic representation of co-polarized and cross-polarized components of the electric field vector in AVA and BAVA [30].

Table 1. Comparison of balanced antipodal Vivaldi antennas

Reference	Substrate	Size (mm)	Return Loss (dB)	Gain (dB)	Frequency (GHz)	Application
[26]	RO 4003	101 × 50 × 1.5	−37	8.7–11.5	6–18	UWB
[27]	RT 6002	74 × 44 × 0.508	−30	7.8–10.8	8–16	UWB
[28]	RT 5880	110 × 44 × 3	−58	1–16	2–40	UWB, 5G
[29]	RT 5880	79.9 × 24 × 0.508	−27	10.2–14.5	10–40	UWB
[30]	RO 5880	162 × 140 × 3.15	−30	3–10	0.92–9.7	UWB
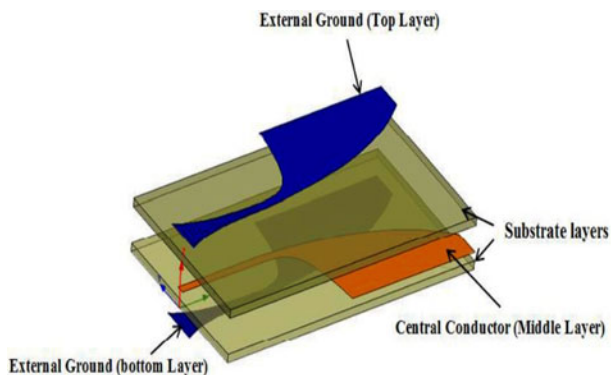
Fig. 6. Structure of balanced antipodal Vivaldi antenna (BAVA) [27].

technologies that assures to revolutionize high data rate transmission. It enables the personal area networking industry leading to innovations and greater quality of services to the end-users.

This technology has been utilized in different attractive applications, such as biomedical detection, ground-penetrating radar, etc. UWB communication systems and UWB indoor positioning systems have achieved significant development due to appealing characteristics in high-speed transmission rate and high multipathway resolution. Nowadays Vivaldi antenna gained considerable attention due to some attractive features such as planar structure, easy fabrication which is widely used for UWB applications.

Because of its low cost and ease of integration, Vivaldi antenna is one of the best candidates used in most of the modern-day UWB applications. However, some of the antennas suffer from a large structure, high cross-polarization, feeding transition limitations as well as high sidelobe level.

The antenna shown in Fig. 8 is used in UWB application. In this design [33], two circular-shaped loads are added on two arms of the antenna, as shown in Fig. 8(b). Slots of different lengths are etched on both arms of the antenna to improve radiation pattern and directivity of the antenna, as shown in Fig. 3(c). The tapered slots are expressed as:

$$x = \pm\{w_0 - 0.5w_0 \exp(\alpha y)\}. \tag{2}$$

For the top and bottom layers, where w_0 is the width of the microstrip line and α is the exponential transition rate. The cut-off wavelength of the antenna depends on the aperture width of the antenna which can be expressed as

$$\lambda_c = 2w, \tag{3}$$

where w is the aperture width of the antenna and λ_c is the cut-off wavelength. The circular shape of flare with slots enhances bandwidth and low-frequency performance of the antenna. In [34], a dielectric cover made of Teflon (PTFE) with relative permittivity of 2.1, loss tangent of 0.0002, and thickness of 0.8 mm is used to make the AVA appropriate for different wideband applications.
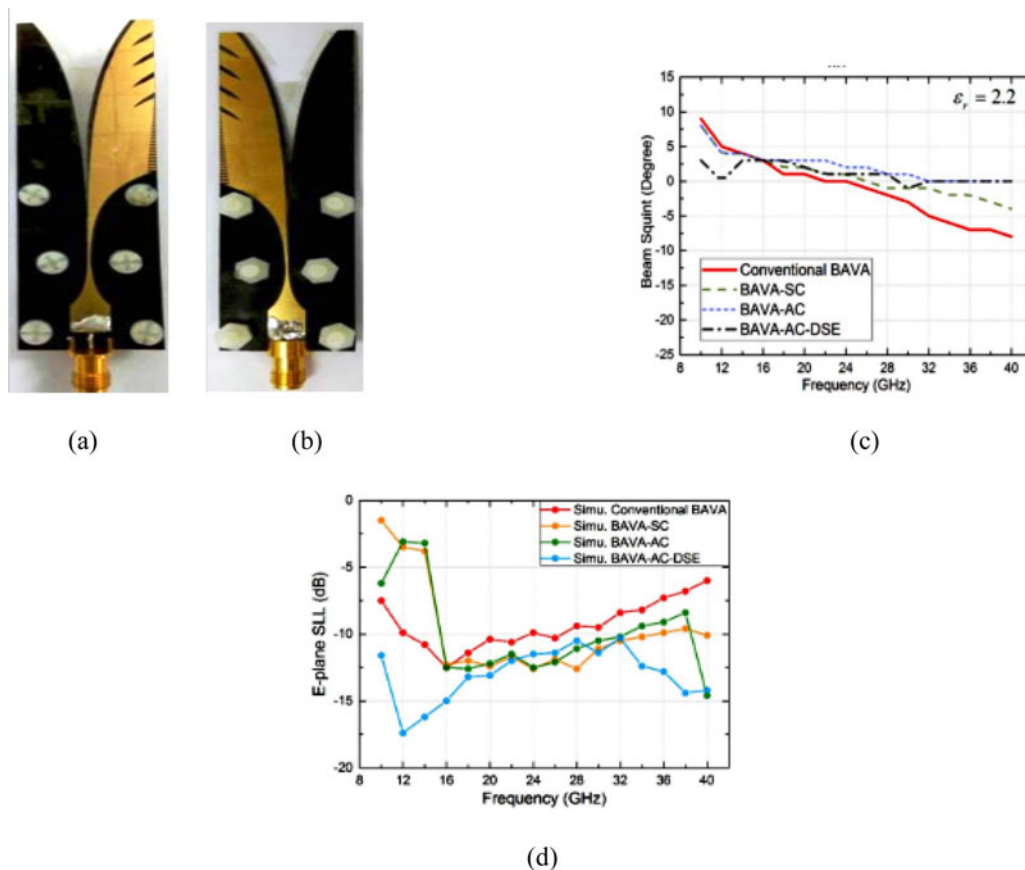
Fig. 7. Effect of balanced AVA. (a) Front view, (b) back view, (c) beam squint, (d) side lobe level (SLL) [29].
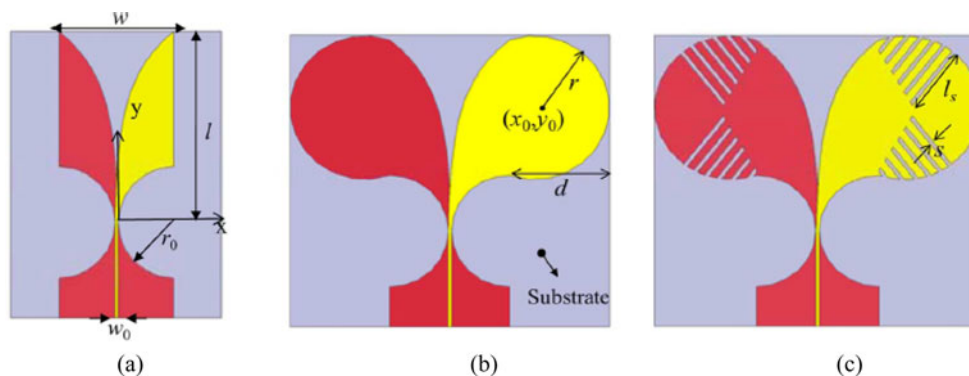

Fig. 8. Vivaldi antenna used in UWB application [33] with $w_0 = 0.675$ mm, $r_0 = 11.6$ mm, $l = 40$ mm, $w = 24$ mm, $d = 20$ mm, $(x_0, y_0) = (16.559, 25.8)$, $s = 0.9$ mm, $l_s = 13.7$ mm.

Due to this innovative design, the proposed antenna offers wider bandwidth, higher gain, lower sidelobe and cross-polarization levels, narrow E-plane half-power beamwidth, and improved F-to-B ratio. In [35], an AVA is presented for wideband application. In this design, dual tapered slot edge is placed on both the arm of the antenna. Due to these slots, the antenna provides wide operating bandwidth, H-plane quasi-omnidirectional radiation pattern at lower frequency band and more directive radiation pattern in the E-plane at the high-frequency band. In [15], a Vivaldi antenna for switchable and widely tuneable band-notch characteristics is proposed. In this design, one stepped-impedance resonator (SIR) is placed to achieve notched band and to achieve tuneable band-notch, varactor diodes are loaded. By controlling the DC bias voltage, the UWB notched band is achieved from 3.1 to 6.8 GHz. In [29], a BAVA is proposed with an asymmetric substrate cut out and dual-scale slotted edges to eliminate the drawbacks of AVA and for different millimeter-wave applications. This design reduces the sidelobe and cross-polarization level, enhancing the gain of the antenna. In [31], a wideband conformal end-fire antenna array mounted on a cylindrical structure provides ultra-wide bandwidth, low cross-polarization level, and wide 3 dB beam width. The effects of the

antenna height with respect to the edge of the hollow conducting cylinder and slant angle of mounting the antenna elements on the conducting surface, on the radiation pattern of the antenna have also been examined. Array assembly offers high gain but side lobes are more and mutual coupling between array elements increases [36]. So different methods for reducing mutual coupling are essential to be employed [37].

In [5], tapered slot edge with resonant cavity structure is used in antenna design to improve the radiation performance of the antenna. Due to this structure, the operating bandwidth is increased by 14.6%. This structure also enhances the gain of the antenna at lower frequencies. In [6], elliptically shaped strip conductors are used in the antenna design to extend the lower operating frequency to enhance the radiation performance of the antenna and make the antenna suitable for wideband communication. The radiation performance of the antenna is also improved in the lower operating band by two pairs of tapered slots and circularly shaped loads. The lower cut-off frequency f_0 of the antenna can be determined using the following equation [6]:

$$f_0 = \frac{c}{w_p \times 1.5 \times \sqrt{\varepsilon_r + 1}}. \tag{4}$$

Here, w_p represent the width of the two arms of the antenna, ε_r is the dielectric constant of the proposed antenna. In [38], a conventional antipodal Vivaldi for UWB wireless communication is presented. Two slots are etched on the ground plane to achieve wider bandwidth, and to increase the bandwidth further, circular grooves as electromagnetic band-gap structure are engraved on the antenna design. Double layer of Vivaldi antenna ground plane is used to enhance the gain of the antenna. A parasitic meander-shaped structure is introduced in the antenna to make the Vivaldi antenna appropriate for UWB application, as given in [39]. The antenna provides bandwidth from 4.5 to 12 GHz. A PIN diode is introduced in the structure to add or remove the UHF bands. In [7], microstrip to tapered transition feed structure Vivaldi antenna is presented. An L shape structure is etched on the radiation fins to enhance the bandwidth of the antenna and make the antenna suitable for UWB communication. A compact AVA for UWB application is presented [40]. It provides low cross-polarization level and good gain over the entire frequency range. In [8], a tapered slot AVA is designed. In this design, elliptical strip conductors are used in feeding structure. Due to this, the antenna becomes an appropriate candidate for UWB applications. This antenna also offers directional radiation in end-fire direction. The comparison between different Vivaldi antennas used in UWB application is given in Table 2.

Dispersion characteristics of Vivaldi antenna for wideband applications

Besides return loss and radiation efficiency, the dispersion characteristic is one of the most important factors which should be considered in wideband applications. In contrast, the conventional parameters are sufficient to evaluate the performance of a narrowband antenna. Still, in the wideband applications, these parameters are inadequate for the applicability of the antenna. The wideband antenna transmits pulses with distortions, and the antenna performance should be evaluated using dispersion parameters, i.e. transfer function, group delay, and fidelity factor as well. The dispersion characteristics of a Vivaldi antenna can be calculated by proper transmission/reception setups. The

Table 2. Comparison of different Vivaldi antennas used in wideband application

Ref No.	Dimension (λ_0)	Bandwidth (GHz)	Gain (dB)
[33]	1.44 × 2.4	5–50	20
[34]	4.74 × 16.5	2–12	10.5
[35]	2.59 × 3.24	5.5–50	2.5–17
[15]	5.5 × 4.4	2.7–20	5
[29]	7.73 × 2.32	3.1–10.6	4–7
[31]	2.814 × 1.05	10–40	9.6–15
[5]	154.8 × 90	0.5–6	1–8
[6]	13.5 × 14.025	2–17	6–11
[38]	22.4 × 3.6	1.5–7.5	6–17
[39]	2.68 × 3.015	4.5–12	4–7
[7]	3.402 × 2.916	3.7–18	2–7

frequency-domain dispersion characteristics of the antenna are the transfer function (S_{21}) and group delay. In *Tx/Rx* setup, the received signal spectrum is attained as follows [41]:

$$S_r(f) = S_{21}(f) \cdot S_t(f), \tag{5}$$

where $S_t(f)$ is the transmitted spectrum and S_{21} is the transfer function of the signal. With a weak distortion in the magnitude and phase of the transfer function, the received signal will have less dispersion. The phase distortion can be estimated by representing the group delay parameter as $-d\phi/df$ where ϕ is S_{21} phase. A nearly constant group delay leads to the linearity of phase. In *Tx/Rx* setups, two antennas should be oriented in a specific direction, as shown in Fig. 9(a). It is due to this fact that the Vivaldi antenna is an end-fire directive antenna and the propagation takes place from the slot surrounded by two radiation elements. Two similar antennas are placed at a separation distance of 60 cm. The 60 cm distance (at the lowest operating frequency approximately 6λ) is selected to have each antenna within the far-field region of the other one. The simulated/measured transfer function and group delay of the Vivaldi antenna are illustrated in Figs 9(b) and 9(c), respectively. The measurement and simulation results are observed to be in good agreement with one another. Furthermore, the behavior of S_{21} and group delay is seen to be acceptable in the required frequency range of 3.1–10.6 GHz.

The time-domain characteristic [41] of Vivaldi antennas being one of the most important factors has been analyzed here. In Fig. 10, the transmitted and received signals of the Vivaldi antenna have been represented where the shapes of the pulse show that the transmitted pulse distortion is not considerable. The amount of pulse distortion induced by the antenna can be validated by the fidelity factor (F) between the received signal and the transmitted signal which is defined by:

$$F = \max_{\tau} \frac{\int_{-\infty}^{+\infty} S_t(t) S_r(t - \tau) dt}{\sqrt{\int_{-\infty}^{+\infty} |S_r(t)|^2 dt . \int_{-\infty}^{+\infty} |S_t(t)|^2 dt}}, \tag{6}$$

where $S_t(t)$ and $S_r(t)$ are the transmitted and received signals, respectively. F represents the similarity between two signals.
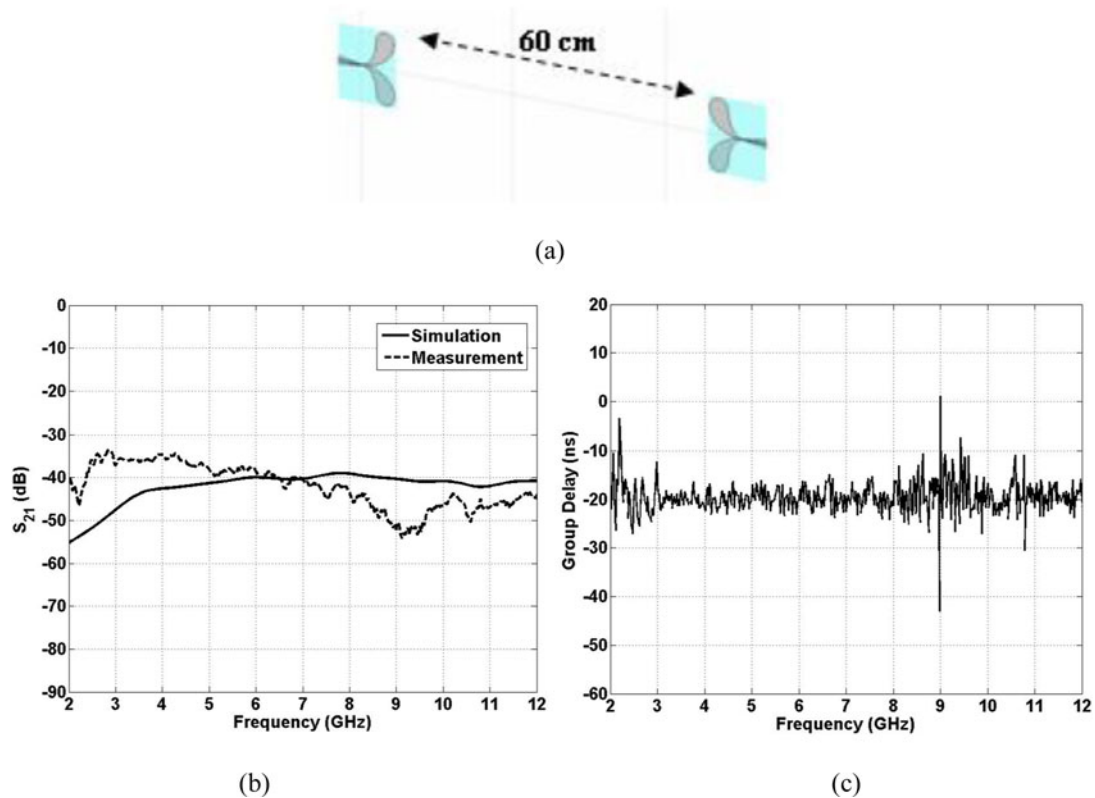
Fig. 9. Simulation setup and transfer function for Vivaldi antenna. (a) *Tx/Rx* setup, (b) magnitude of S_{21}, (c) group delay [41].
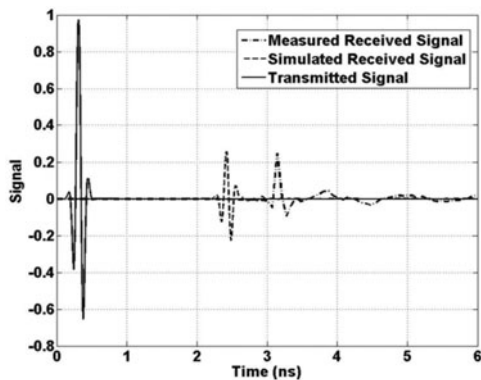

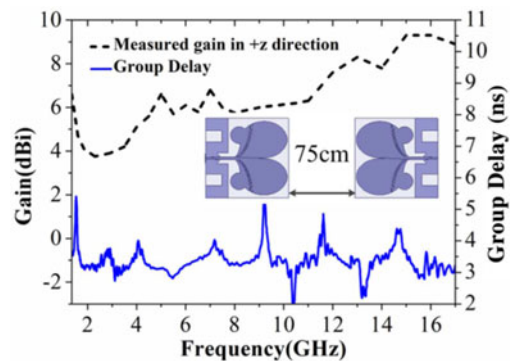Fig. 10. Transmitted and received signals in *Tx/Rx* setup [41].

Fig. 11. Measured gain in end-fire direction and group delay [6].

With two similar signals, F coefficient becomes unity. Using equation (6), the fidelity factor between transmitted and received signals in *Tx/Rx* setups between two identical antennas has been calculated [41] which yields a fidelity factor of 0.7904. As we know, because the Vivaldi antenna has no omnidirectional applications [1], the transmission/reception performance of the antenna in one direction has been considered.

Two identical proposed AVAs in this letter [6] are placed face to face with a distance of 75 cm, as shown in Fig. 11. The measured group delay varies around 3.4 ns with a fluctuation of 0.6 ns in most frequencies, which means this antenna can transmit and receive signals without severe distortion in the whole operating band.

Dispersion characteristics of a compact AVA [7] in terms of group delay are measured and shown in Fig. 12. Almost flat response is noticed over the operating bandwidth, which indicated minimal distortion in the transmitted pulse.

In [40], a compact AVA for UWB applications is proposed. Both the plots in Fig. 13 show the dispersion characteristics of the antenna with a discontinuity at 3.55 GHz, possibly due to the resonance at that frequency in the operating bandwidth.

The simulated time-domain response of a UWB antipodal TSA [8], when excited with a Gaussian pulse covering the entire frequency spectrum, can be observed in Fig. 14 [8]. The received pulse was obtained by placing an E-field probe in the far-field of the antenna at 10 m oriented along the *x*-direction. The originally
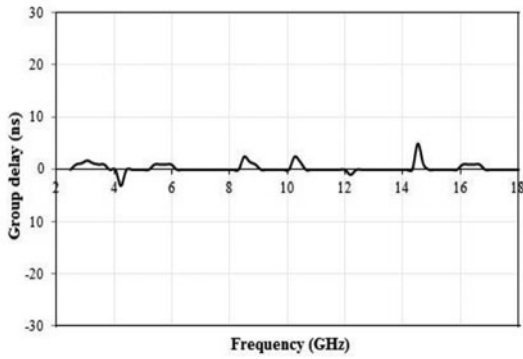
Fig. 12. Measured group delay [7].

Fig. 14. Simulated transmitted pulse and received pulse on the E-field probe at the far-field of the antipodal TSA [8].

transmitted pulse full-width at half-maximum (FWHM) was 180 ps, while the received pulse on the x-oriented E-field probe had an FWHM of 187 ps. The fidelity factor was calculated at 0.94.

Fractal-based Vivaldi antenna

Fractal is a structure which is repeated but not predefined [42]. This type of construction consists of multiple self-copies at various levels. Using fractal geometry, the space occupied by the antenna can fill in a more effective manner than any traditional Euclidean antenna. For example, we have discussed the geometric construction of the standard Koch curve, which is simple that starts with a straight line as an initiator. Then it is partitioned into three equal parts, and the segment at the middle is replaced with two others of the same length which is the first iteration of the geometry which is called the generator [k_0]. This process is reused in the generation of higher iterations where successive iterations contain a smaller bump on each side of the first bump, and the sides of every triangle are same. Figure 15 shows different iterations Koch fractal shape for a given indentation angle "θ" where the indentation angle "θ" is taken as a design parameter and its value is chosen as 60° for conventional Koch fractal curve.

The dimension of the Koch fractal geometry can be calculated by the following equations [42]

$$S_1 = S_4 = \frac{L_0}{3} \qquad (7)$$

Fig. 15. Steps for construction of conventional Koch curve geometry [42].

$$S_2 = S_3 = L_0\left(\frac{1}{2} - \frac{1}{3}\cos\theta\right). \qquad (8)$$

The perimeter after n^{th} iterations is:

$$L_{perimeter}^n = 4\left[\frac{2}{3}\left(\frac{5}{3} - \cos\theta\right)\right]^n L_\theta, \qquad (9)$$

where L_θ is the side of the generator.

AVA with Koch shape fractal on radiator and ground is shown in Fig. 16. In [43] to make the antenna suitable for different

Fig. 13. (a) Phase response of the fabricated FR4 antenna. (b) Group delay of the fabricated antenna [40].

Fig. 16. Antipodal Vivaldi antenna with fractal structure. (a) Antenna structure with $a = 4.03$ mm, $b = 11.17$ mm, $c = 18.15$ mm, $d = 23.02$ mm, $e = 59.81$ mm, $f = 7.00$ mm, $g = 9.97$ mm, $h = 1.00$ mm, $i = 1.00$ mm, $r = 13.12$ mm, $w_1 = 36.30$ mm, $w_2 = 21.35$ mm. (b) Current distribution [43].

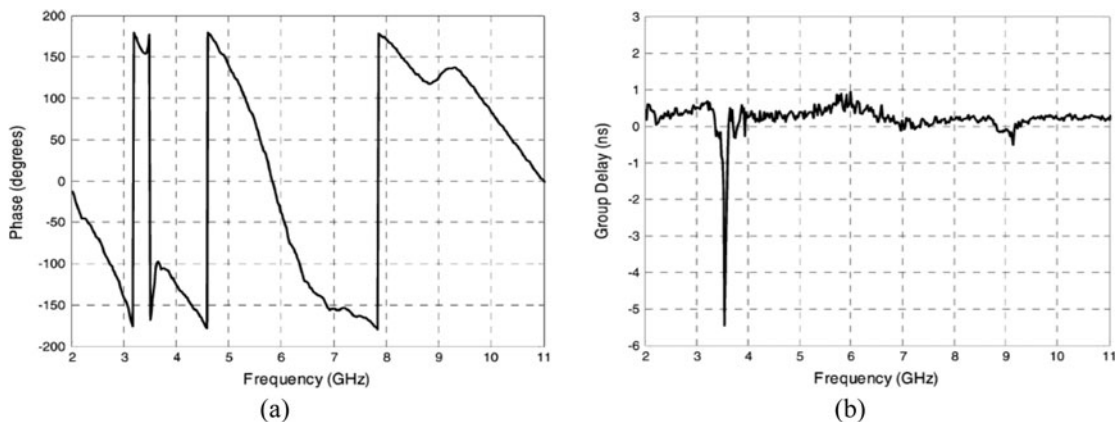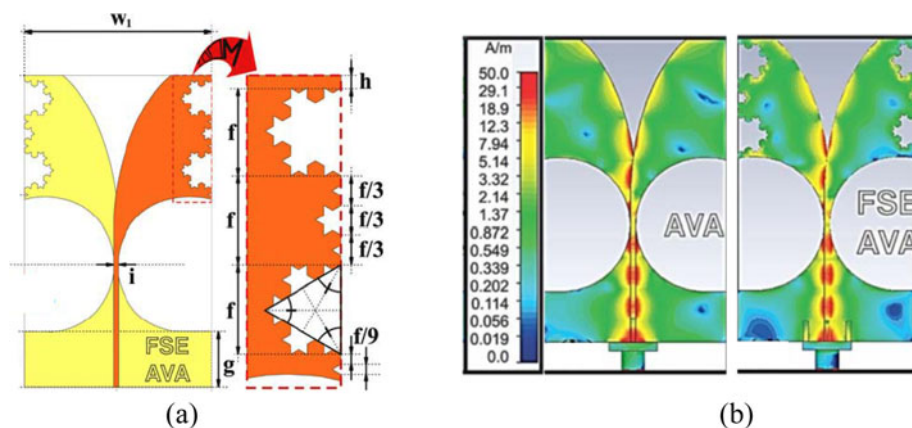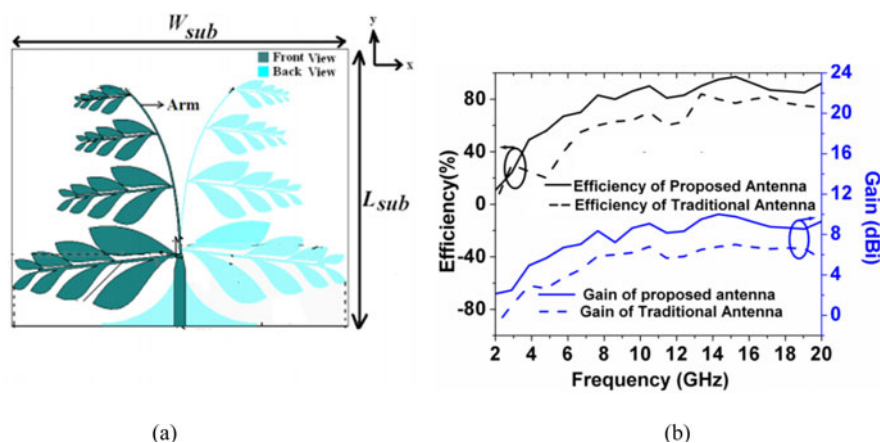**Fig. 17.** (a) Antipodal Vivaldi antenna with a fern-inspired fractal structure with $L_{sub} \times W_{sub} = 50.8 \times 62 \times 0.8$ mm^3. (b) Gain improvement using fractal structure [10].

medical imaging applications, the Koch fractal structure is used in the radiator and ground plane of the antenna. Due to the presence of fractal slot edge, the lateral E-fields are suppressed in the surroundings of the fractal structure because the fractal slot edge makes the interface between the metal edge and medium become softer. Figure 16(b) shows the surface current distribution of AVA and fractal slot edge AVA. The presence of the fractal structure on the edge of the antenna rejects the trapping of E-field, which is observed in the AVA. The presence of fractal-shaped ellipse structure in AVA improves the gain of the antenna over the entire frequency range, which makes the antenna an ideal candidate for different UWB and imaging applications.

In [10], a new type of fractal structure known as fern leaf fractal structure is applied in the AVA design, as shown in Fig. 12(a).

$$x_1 = \pm (w_0 - 0.75 w_0 \exp (a_1 y_1)). \tag{10}$$

Equation (10) is used to design the radiator and ground plane of the antenna. Where w_0 represents the width of the feed line and a_1 denotes the rate of tapering given in equation (6)

$$a_1 = \frac{1}{L_1} \ln \left(\frac{w_0 + 0.75 L_d}{0.75 w_0} \right). \tag{11}$$

In equation (11) L_1 is the radiator length and L_d is the flared distance. In Fig. 17(a) L_{sub} and W_{sub} represent the length and width of the antenna, respectively. In the antenna structure, θ_1

Table 3. Comparison of different fractal-based Vivaldi antennas

Ref No.	Dimension (λ_0)	Bandwidth (GHz)	Gain (dB)
[43]	2.14 × 3.53	5.08–12	8.5
[10]	7.62 × 9.30	2–20	10
[44]	13.206 × 4.686	4.2–42	13.9

and θ_2 represent the rotation angles. The second iteration of this fractal structures improves the bandwidth of the antenna by reducing the lower cut-off frequency. The proposed antenna also provides a fractional bandwidth of 175%. The designed antenna also produces higher gain over the entire frequency range, as shown in Fig. 17(b). In [44], a novel fractal inspired AVA is proposed for wideband applications. First, a parasitic fractal lens is introduced in the flare aperture section of the AVA to improve its performance. But the presence of parasitic lens does not influence the performance of the antenna at a higher frequency range. Now to adjust the gain and radiation pattern of the antenna at high frequencies, a Koch fractal shape dielectric director as an extension of the antenna substrate is used to improve the gain of the antenna.

The comparison of different fractal-based Vivaldi antenna is given in Table 3. The fractal structure makes the antenna layout complex. Still, the presence of the fractal structure makes the antenna innovative as well as improves the radiation performance
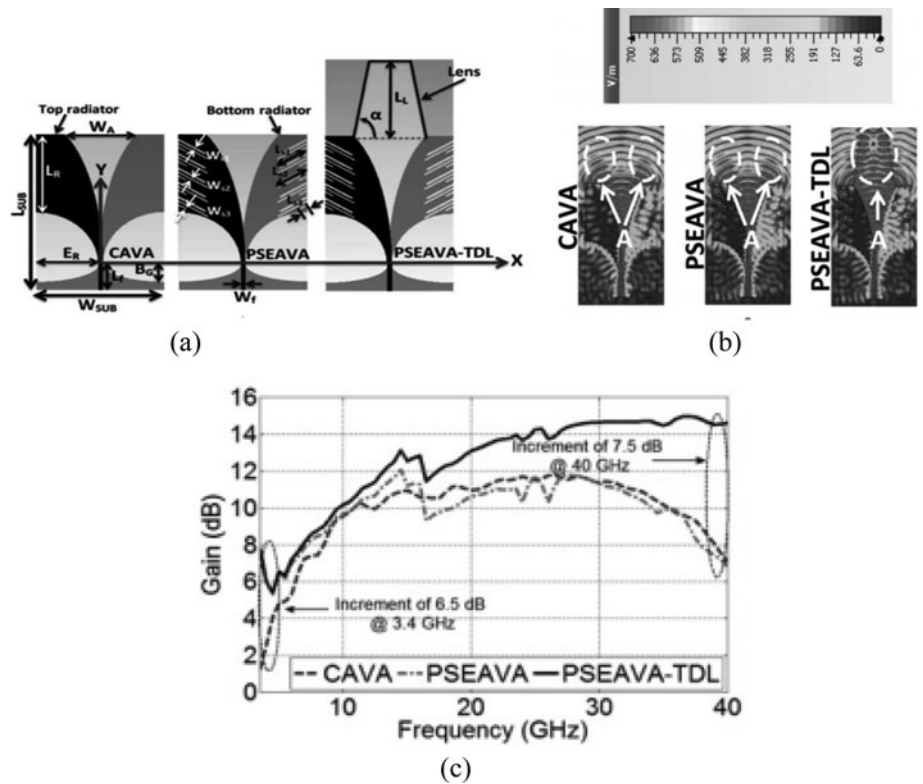
Fig. 18. Antipodal Vivaldi antenna for imaging application. (a) Antenna structure with $L_{SUB} = 60$ mm, $W_{SUB} = 40$ mm, $L_R = 30$ mm, $B_G = 6.80808$ mm, $L_f = 10$ mm, <ddollar><ddollar> $E_R = 19.405$ mm, $W_A = 22.84$ mm, $L_L = 30$ mm, $W_f = 1.19$ mm, $d = 78.71°$, $W_{s1} = 0.8$ mm, $L_{s1} = 9$ mm, $W_{s2} = 0.6$ mm, $L_{s2} = 9.8621$ mm, $W_{s3} = 0.6$ mm, $L_{s3} = 2.84615$ mm, (b) electric field distribution, (c) gain characteristics [45].

of the antenna without occupying more geometrical area. The advantages of using fractal shape in the antenna design are that it enhances the performance of the antenna without increasing antenna dimensions. The fractal layout on the edge of the radiator and the ground plane of the Vivaldi antenna reduces the sidelobe level and also improves the directivity.

Vivaldi antenna for microwave imaging application

Nowadays, microwave imaging [45] technique is widely used in different detection application. In this imaging technique, first, a microwave signal is transmitted to the targeted object. Then the signals reflected from the object are tested to reconstruct images of the targeted objectives. In this application, the antenna plays a vital role with high directivity, and improved radiation characteristics are used.

The antenna design, as shown in Fig. 18, is used for imaging of different construction materials [45]. In this design, a trapezoidal shape dielectric lens, as shown in Fig. 18(a) is used in the aperture of the antenna to improve radiation properties making it suitable for imaging of different construction materials. Figure 18(b) shows the electric field distribution of the proposed antenna. The presence of the trapezoidal shape dielectric lens concentrates most of the electric field in the desired direction, i.e. along the *y*-axis direction. The improvement of the gain of the antenna due to the presence of a dielectric lens is given in Fig. 18(c). In [46], rectangular-shaped slits are introduced on the radiator and ground of the antenna to achieve wide impedance bandwidth. A half-circular shape dielectric lens is also introduced in the antenna design to achieve high directivity and front-to-back ratio. Due to these features, the antenna is appropriate for imaging of cracks inside concrete. A corrugated Vivaldi antenna is proposed in [11] for microwave imaging applications. In this

design, due to the presence of grooves, the antenna provides improved radiation performance. In [47], a Vivaldi antenna with a corrugation structure on the radiating portion is presented. In this design, grating elements are also loaded near the tapering part of the antenna to achieve higher gain and improved radiation pattern in the end-fire direction. Due to these features, the antenna can be used in microwave imaging. In [48], a novel Vivaldi antenna with several slots etching on the radiation fins is presented. These slots reduce the size of the antenna and also provide wider bandwidth, higher gain, and improved directivity. The slots also make the antenna highly efficient. Due to its compact structure and attractive features, the antenna is used in different medical imaging applications. In [49], a balanced AVA is presented for microwave imaging applications. In this design, exponentially tapered corrugation edge and elliptical shape director is used to enhance the radiation characteristics. The elliptical shape dielectric director improves the gain of the antenna over the entire frequency range and also produces a directive radiation pattern which makes it appropriate for an imaging application. An AVA in [12] is proposed for detecting void inside the concrete. Here, to improve the gain of the antenna at high as well as lower frequencies, rectangular shape slit and a dielectric director of half elliptical shape are used in the antenna design.

The proposed antenna is used to obtain the depth of penetration of concrete specimen and wideband microwave imaging application, as demonstrated in Fig. 19. The antenna is attached to the scanning machine keeping a particular gap to obtain the 3D and 2D images of the specimen. These specimens are generated using data and synthetic-aperture-radar-based algorithm. In this case, one of the 3-month-old concrete beams is used as a specimen to simulate the void, as shown in Fig. 19(a). The sample is scanned by using a 3 mm step size. The holographic slices of the 3D images are shown in Figs 19(b)–19(d).
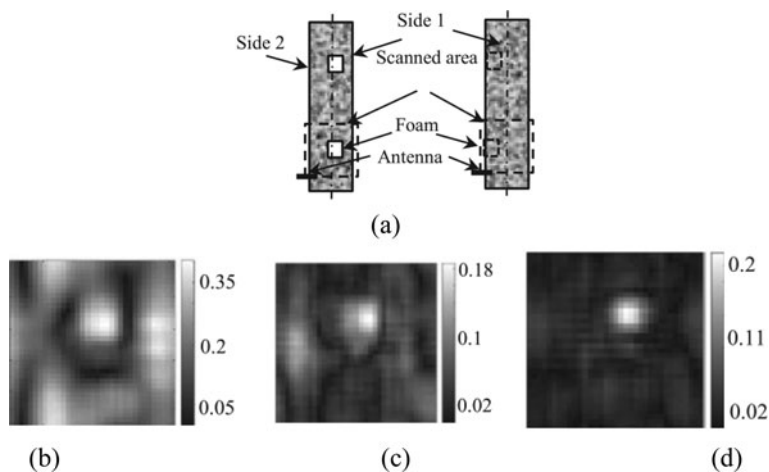
Fig. 19. Proposed antenna test the concrete beam: (a) top and side view; holographic slices of 3D images: (b) the top of insert, (c) 9 mm below the top insert, (d) 15 mm below the top insert [12].
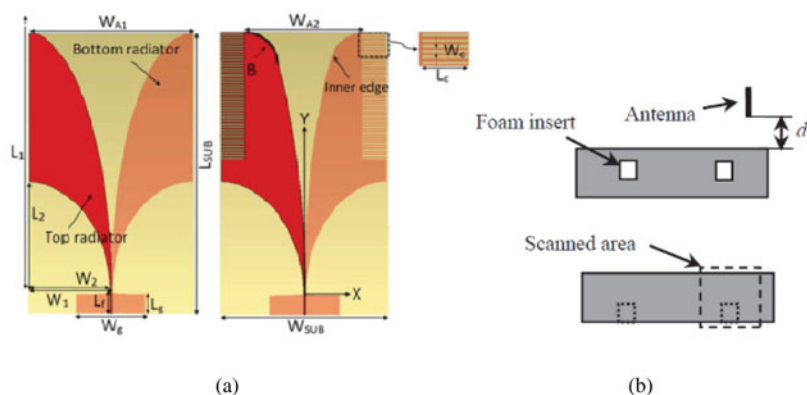
Fig. 20. (a) Conventional antipodal Vivaldi antenna and comb-shaped slits antipodal Vivaldi antenna with $W_{SUB} \times L_{SUB} = 120 \times 202$ mm^2, $W_{A2} = 84$ mm, $W_2 = 59.43$ mm, $L_1 = 229$ mm, $L_2 = 80$ mm, $W_f = 1.14$ mm, $L_f = 15$ mm, $W_g = 50$ mm, $L_g = 15$ mm, $W_c = 1$ mm, $L_c = 17$ mm, $B = 25$. (b) Schematic of concrete beam with two foam inserts imaged by the proposed antenna at standoff distance d [$d = 10$ mm] [50].
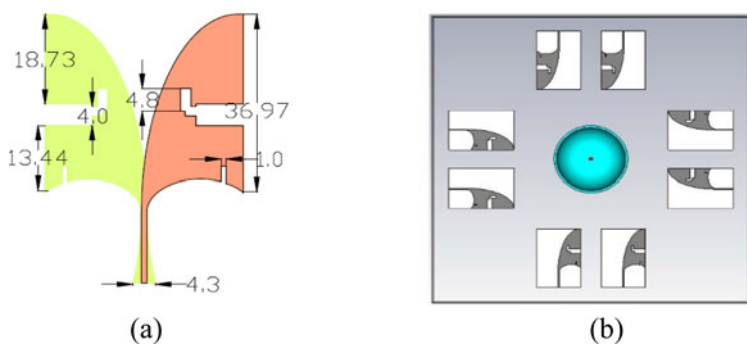
Fig. 21. (a) Single parametric antenna [dimensions in "mm"]. (b) Antenna array surrounding the breast with the tumor in it [52].

In [50], an elliptically-tapered AVA with an operating frequency range from 1.65 to 18 GHz designed for microwave imaging applications is presented. It includes comb-shaped slits and elliptical opening in the top and bottom radiators. It is shown that the antenna gain has been increased by comb-shaped slits at lower frequencies up to 9.5 dBi at 2 GHz and at higher frequencies up to 14.2 dBi at 18 GHz. Comb-shaped corrugation on elliptical flare is applied in [51] to efficiently find empty spaces in the concrete beam. The corrugation on flares increases gain and return loss of the AVA (Fig. 20).

In [52], the design and implementation of a Vivaldi antenna (BAVA) and breast phantom for breast cancer imaging have been covered within the range of 3.1–10.6 GHz. Two different phantoms are made to simulate the scene. A dielectric constant relatively close to the real breast tissues has also been found.

This design can be used in breast cancer detection without the need for any liquid coupling medium, which is required in many other applications (Fig. 21).

In most of the cases, Vivaldi antennas play an essential role for imaging applications though in some of the issues it suffers from the deviated beam (E-plane) at upper frequencies as well as increased sidelobe levels at mid frequencies (Table 4).

## Gain boosting techniques in Vivaldi antennas

Using dielectric director

Different researchers use a high permittivity dielectric material in the aperture center of the antenna known as dielectric lens or director to achieve wider bandwidth and higher gain [53].

Table 4. Comparison of different Vivaldi antennas used in microwave imaging applications

Ref No.	Dimension (λ_0)	Bandwidth (GHz)	Gain (dB)
[45]	2 × 3	6–40	8–14.8
[46]	3.52 × 5.28	3.4–40	6–13
[11]	9.486 × 7.65	1.96–8.61	5.6–10.4
[47]	4.635 × 4.12	2.9–11	6–8.2
[48]	4.5 × 5.3	3.0–6.5	5.5–7.5
[49]	14 × 21.6	1.5–15	1–14
[12]	28.8 × 30	1–30	2.2–11

Table 5. Comparison of Vivaldi antennas with dielectric director

Ref No.	Dimension (λ_0)	Bandwidth (GHz)	Gain (dB)
[49]	14 × 21.6	1.5–15	1–14
[12]	28.8 × 30	1–30	2.2–11
[55]	33.09 × 24.66	1–14	1–12
[56]	8.625 × 9.105	2–40	1–13
[57]	3.52 × 5.28	3.4–40	4–14.8
[58]	4.98 × 3.75	4–30	7–9
[13]	3.366 × 1.584	3.01–10.6	3.42–7
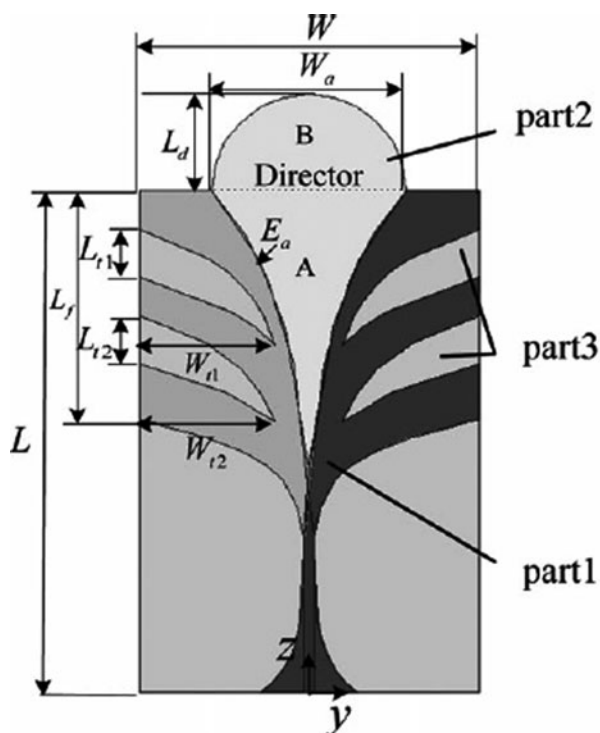
Fig. 22. Antipodal Vivaldi antenna with dielectric director having L = 108 mm, W = 70 mm, W_a = 42 mm, L_d = 32 mm, L_f = 72 mm, L_{t1} = 13.5 mm, L_{t2} = 11.8 mm, W_{t1} = 26 mm, W_{t2} = 26.5 mm [49].

This method is also used in [49] where a half circular-shaped lens is used for gain enhancement, as shown in Fig. 22. The proposed antenna also used exponentially tapered corrugation slot edge on the radiator and ground plane. The presence of the rectangular shape slot edge and the director helps the antenna to achieve wider bandwidth, high directivity, and front-to-back ratio. The tapered slots also reduce co-polarization and cross-polarization [54].

In [12], an exponential tapered AVA with a half elliptical-shaped dielectric lens as an extension of antenna substrate is used. The presence of this dielectric lens improves the gain of the antenna, and a regular slit edge extends the lower end bandwidth of the antenna to find application in different UWB applications. Hemisphere shape lens loaded in the antenna structure for different time-domain operation is given in [55]. This hemisphere shape lens increases overall directivity of the antenna and also widens the bandwidth of the antenna. A trapezoidal shape dielectric lens is loaded in the major axis direction in [56]. The presence of the dielectric director overcomes the shifting of the antenna peak gain problem and enhances the radiation performance of the antenna. In [57], a trapezoid shape dielectric director and periodic slit edge are introduced in the antenna to improve the radiation properties of the antenna. The high permittivity dielectric director reduces mutual coupling between the elements and beam tilting problem and concentrates the radiation in the end-fire direction. As a result, the antenna produces improved gain with the dielectric director.

A high permittivity material known as a director is used in [58] to improve the radiation performance of the antenna. This director focuses most of the energy toward the aperture center and significantly improves the gain and directivity of the antenna. In [59], a Vivaldi antenna with triangular shape dielectric lens is presented. In this design, due to the dielectric lens, the electrical path length is increased and transmitted wave delayed. Due to this delay, the radiated wave becomes parallel and produces more directed radiation pattern and improved gain. In [13], a director and a convex lens are added in the wideband AVA design to improve the performance of the antenna at high frequencies. By using the dielectric lens with other performance improvement techniques like an array, slots, corrugation, etc., enhances the parameters of AVA very effectively [60]. The comparison of Vivaldi antennas with a dielectric director as the gain booster is given in Table 5. In most of the cases, dielectric directors found suitable for enhancing the antenna characteristics but achieving an appropriate shape of the director may be a challenging issue that can lead to the bulky structure of the antenna along with higher fabrication cost.

Using dielectric slab

Dielectric slab placed on both sides of the antenna is a practical approach to enhance the gain of the Vivaldi antenna [61] but with a slight compromise of increasing antenna dimension. The dielectric slabs utilize the coupling between the antenna and dielectric sheets to overcome problems such as main beam tilt and split, high cross-polarization component, and low gain at high frequencies narrowing its gain bandwidth.

In [61], an innovative antipodal tapered slot antenna with double thin rectangular dielectric sheets (Fig. 23) is presented to achieve improved radiation properties. In [62], a simple dielectric slab placed on both the side of the Vivaldi antenna is proposed for improving the performance of the antenna. The dielectric slabs
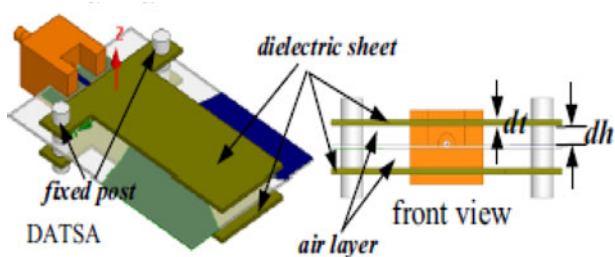
Fig. 23. Antipodal Vivaldi antenna with a dielectric slab [61].

Fig. 25. Geometry of antipodal Vivaldi antenna with bandpass filter [14].

Table 6. Comparison of Vivaldi antennas based on a dielectric slab

Ref No.	Dimension (λ_0)	Bandwidth (GHz)	Gain (dB)
[61]	3 × 2	6–40	8–14.8
[62]	4.472 × 5.504	3.5–16.5	5.72–15.3

match space waves which are emitted from the CVA and then converted into surface waves which radiate in the end-fire direction. By using this method, the gain of the antenna increases without elongating the overall antenna length. Comparison of Vivaldi antenna design based on a dielectric slab is given in Table 6.

Using parasitic lens

Different researchers have found that the herein method [63] can be used to enhance the gain of the antenna. In this method, by introducing a parasitic element in the flare aperture section of the antenna, the gain is increased by focusing the radiation in the end-fire direction.

It is seen from Fig. 24 that a parasitic element is placed in the aperture section of a conventional AVA and it improves the field coupling between the arm of the antenna; as a result, it produces stronger radiation in the end-fire direction [63]. By using this technique, the directivity and the high-frequency performance of the antenna are improved. The most important part of the broadband antenna is its long electrical length, but it reduces the performance of the antenna at higher frequencies due to phase reversal along the length. As shown in Fig. 19(b), due to phase reversal, off-axis radiation is created along with end-fire radiation from the aperture of the antenna. This problem of the broadband antenna can be overcome by minimizing the flaring
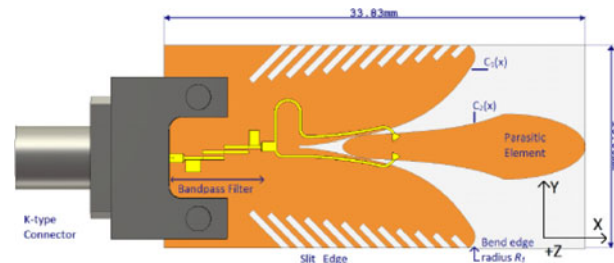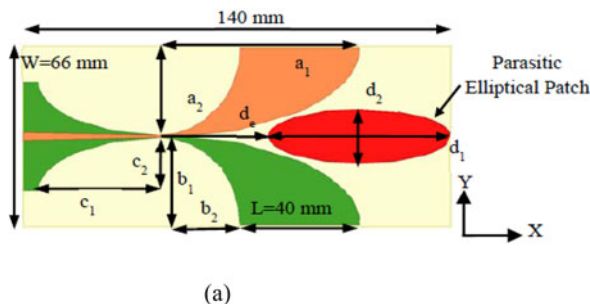
length of the antenna. This reduction in the flare length enhances the lower operating frequencies.

In [64], an AVA with diamond shape parasitic lens is presented to improve the high-frequency gain. The presence of the lens enhances the radiation performance of the antenna at higher frequencies. In [65], an elliptical-shaped parasitic element is introduced to reduce the sidelobe radiation and improve the directivity of the antenna. The presence of this element enhances the directivity and gain of the antenna. In [28], a Vivaldi antenna is presented where a metal director is used to improve the gain and radiation pattern of the antenna. The presence of the director enhances the bandwidth of the antenna.

A dual-stub coplanar Vivaldi antenna with a parasitic element placed in the throat area and an integrated bandpass filter is shown in Fig. 25 [14]. The exponential curve applied to design the antenna is $C_{i(x)} = \pm a_i \times e^{p_i x}$ where $C_{i(x)}$ is the exponential profile with $a_i = 0.15$ and $p_i = 0.25$. The presence of two semi-elliptical-shaped exponential curves with a parasitic element in the throat of the antenna structure provides better radiation performance. The slits present on the edge of the radiator and ground plane regulate the radiation performance of the antenna. In order to suppress the harmonics, the bandpass filter is introduced in the source end. The dependence on permittivity and thickness of dielectric material makes a constraint for the designers. Also, a dielectric lens slightly increases the weight. Comparison of the Vivaldi antenna design using the parasitic lens is given in Table 7.

Vivaldi antenna with metamaterial

Metamaterials [66] have some unique characteristics than those of other natural materials. It is a synthetic type of material which depends on structure such that it discloses some properties which are not usually found in natural materials, mainly a
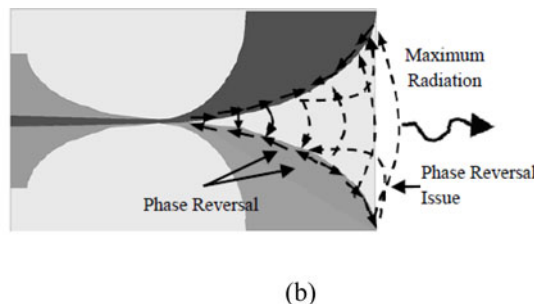

Fig. 24. (a) Antipodal Vivaldi antenna with parasitic lens having $a_1 = 66$ mm, $a_2 = 33$ mm, $b_1 = 32$ mm, $b_2 = 26$ mm, $c_1 = 40$ mm, $c_2 = 20$ mm, $d_1 = 30$ mm, $d_2 = 10$ mm, $d_e = 36$ mm. (b) E-field distribution at high frequencies [63].

Table 7. Comparison of Vivaldi antenna with parasitic lens

Ref No.	Dimension (λ_0)	Bandwidth (GHz)	Gain (dB)
[63]	8.120 × 3.828	5.2–30	−4 to 12.2
[64]	13.268 × 12.412	2.8–12	3–10.5
[65]	9.3 × 3.85	6 −55	0–16
[28]	4.4 × 9.8	3–40	0–13
[14]	0.406 × 0.192	25–30	9.4

Table 8. Comparison of different Vivaldi antenna using metamaterial

Ref No.	Dimension (λ_0)	Bandwidth (GHz)	Gain (dB)
[66]	3.48 × 0.06	5–50	20
[9]	3.8 × 2.1	3–13.9	9.9
[67]	15 × 15	1–20	8.5

negative refractive index. Applications of metamaterials in microwaves are numerous and opened the door to new strategies in the design of microwave devices, also referred to as dispersion engineering, which considers and controls the phase response of devices. There are two main approaches in the design of microwave circuits using metamaterials: the resonant approach which uses thin wires, split-ring resonators (SRRs) and complementary split-ring resonators (CSRRs), and the transmission line approach based on dual transmission line theory. The first one leads to lossy and narrowband circuits, while the second, non-resonant approach, provides design tools for broad bandwidth devices with low loss. Metamaterials are used to improve the radiation properties of the antenna. The anisotropic zero-index metamaterial (AZIM) [67] is used to enhance the gain of the antenna.

In order to achieve a broadband gain, the high index metamaterial and anisotropic inhomogeneous artificial material are used [68]. Many researchers have found an impact on the characteristics of the antenna by using this type of materials. Metamaterial offers some surprising features. In antenna design, either unit-cell or multiple-cell metamaterials are used as an array. A unit cell is usually smaller than 1/10 of the operating wavelength, depending on the shape of the metamaterial, but the unit-cell size is different. The presence of metamaterial reduces the dimension of the antenna as well as improves the radiated power level, enhances the bandwidth and gain of the antenna. By using metamaterial as a radiating component, one can design an antenna of compact size for multiple communication systems. The metamaterial is used as an antenna environment to enhance the radiation properties of the antenna. The metamaterial is also used as part of the antenna component to miniaturize the size of the antenna without disturbing the

performance. But the difficulty lies in designing metamaterial unit cells as well as low EM wave confinement within guiding structure and more moderate gain enhancement at lower frequencies.

As shown in Fig. 26, metamaterials are loaded in the aperture section of the AVA [66]. The presence of the metamaterial unit in the antenna aperture section improves the gain of the antenna in the non-resonant frequency band, as shown in Fig. 26(b) [66]. It can be observed that if the cell length is lower than the gain reduced at higher frequency as well as lower frequency. But when we add rows of metamaterial unit cells, then the gain increases drastically at the non-resonant frequency band. Parallel unit of metamaterials works as a phase shifter and enhance the radiation performance of the antenna. A compact high-gain AVA is presented in [9]. Again, to enhance the main lobe radiation and the gain, the transverse slots are etched on the arm. A band-notched Vivaldi antenna with AZIM unit cell is designed in [67] to enhance the overall gain of the antenna. In addition to the metamaterial unit, a CSRR is also introduced. Due to their presence, the antenna became a good candidate for UWB application. Further, a small size AVA with a modified I-shaped metamaterial is employed in [69]. Signal radiation in undesirable direction can be evaded with an enhanced gain by using metamaterial slabs around AVA [70]. From all these comparisons, we can say that determining the shape and position of metamaterial is a hard task. Table 8 shows the comparison of different Vivaldi antenna structures which used metamaterial for improving the performance of the antenna.

Vivaldi antenna with special structures

The conventional Vivaldi antenna is known for its UWB characteristic, but low directivity. In order to improve the directivity and for extensive applications, some unique methods are used in the
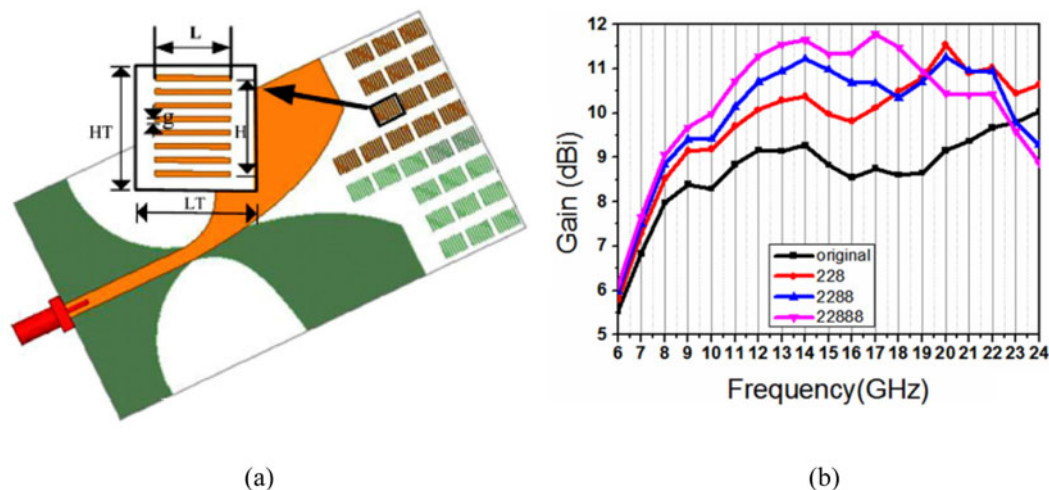
Fig. 26. (a) Antipodal Vivaldi antenna with metamaterial having *LT* = 5.25 mm, *L* = 3 mm, *g* = 0.2 mm, *HT* = 4. (b) Gain boosting using metamaterial [66].
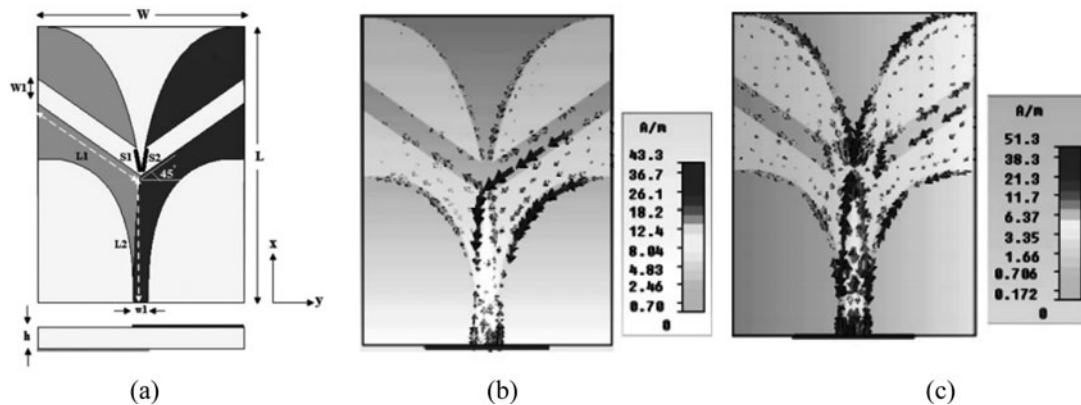
Fig. 27. (a) Dual polarized antipodal Vivaldi antenna with $W \times L \times h = 80 \times 60 \times 1.6$ mm^3. (b) Narrowband current distribution. (c) Wideband current distribution [72].

design of novel Vivaldi antennas. In [71], a Vivaldi antenna with high selectivity and the notched band is presented. An open-circuited half-wavelength resonator and a short-circuited SIR are introduced in the antenna structure to achieve two notched poles inside the stopband. The resonating frequencies are precisely determined to obtain the wider bandwidth. The antenna offers good frequency selectivity in the notched band from 4.9 to 6.6 GHz, and the antenna provides proper impedance matching, higher gain, and excellent directivity.

A dual-mode AVA is presented in [72]. In this design, the antenna operates in wideband and narrowband modes, as shown in Fig. 27, which operates in the UWB spectrum. In this design, a rectangular strip is etched on the radiator by rotating 45° in the counter clockwise direction to achieve narrowband operation. For performing the wideband operation, switches (S_1, S_2) are placed along the tapered side of the antenna to bridge the slot line. When both the switches are in OFF condition, then the antenna performs the narrowband operation, and when both are in ON condition, then the antenna performs the wideband function. The surface current distributions for narrowband and wideband modes are given in Figs 27(b) and 27(c), respectively, to understand the working of the antenna.

In the narrowband operation, the taper section of the antenna is disconnected due to the slot. So, current flows only through the linear slot. On the other hand, in the wideband operation, current flows along the entire taper section of the antenna. The use of rectangular slots in the antenna design provides wideband rejection and enhances the gain of the antenna. The proposed antenna provides higher gain throughout the bandwidth without compromising the gain and impedance performance of the antenna. Again in [73], a Vivaldi antenna is presented with a stepped connection structure used between a slot line and tapered patches. Due to the presence of this stepped connection structure, the antenna provides better impedance matching as well as wider bandwidth. The antenna also offers better gain due to this structure. A novel structure to enhance directivity, end-fire radiation, and to reduce the sidelobe radiation is presented in [16]. Here to restrict the field radiation and concentrate the energy in the end-fire direction, coupling patches are introduced in the aperture area of the antenna. In [17], a Vivaldi antenna is presented where the gain of the antenna is enhanced by adding a via-loaded maple leaf shape on the edge of the radiator and ground plane. These maple leaves increase the gain at the upper-frequency band.

In [18], a three-port Vivaldi antenna is presented for diversified applications for vehicular environment. The given antenna is capable of producing three directional radiation patterns. The lower ECC value and higher directivity gain make the antenna appropriate for automobile applications. Slots with variable capacitors or SRRs are employed to create re-configurable AVA for eliminating unwanted bands in [74].

Conclusion

Vivaldi antenna is one of the most promising candidates for UWB applications due to its wide bandwidth and featured directive radiation characteristics. A thorough review of all Vivaldi antenna performance improvement methods present in most of the literatures has been cited in this paper. These methods are based on the modification based on the physical geometry of an antenna which results in a change in various antenna parameters like size, gain, front to back ratio, bandwidth, radiation pattern, polarization, and operating frequency range. Each technique is discussed in brief with the help of recent research work to prove the impact of a particular technique on antenna parameters. This review work concludes that Vivaldi antenna performance enhancement methods such as slots, corrugation, fractal shapes, dielectric lens, and BAVA can be used to eliminate the undesirable effect of beam squint and cross-polarization. Similarly, the parasitic patch and dielectric lens should be designed such that it will concentrate maximum radiation in the end-fire direction to increase the gain. Furthermore, the designing and positioning of a unit cell of metamaterial on a Vivaldi antenna to enhance its gain, bandwidth, and return loss should be carefully performed. This paper also presents a study of various applications where Vivaldi antenna is used as a critical element. In keeping with this study, the new researchers will be enlightened with all the Vivaldi Antenna performance enhancement methods. They will aid as a guiding principle and reference to applicably select the method while designing an antenna. Lastly, the author expresses regret to the researcher society if any novel contribution in this field is omitted unwittingly during this study.

References

1. **Gibson PJ** (1979) The Vivaldi aerial. *Proceedings of the 9th European Microwave Conference*, pp. 101–105.
2. **Yngvesson K, Schaubert D, Korzeniowski T, Kollberg E, Thungren T and Johansson J** (1985) Endfire tapered slot antennas on dielectric substrates. *IEEE Transactions on Antennas and Propagation* **33**, 1392–1400.
3. **Gazit E** (1988) Improved design of the Vivaldi antenna. *IEEE Proceedings* **135**, 89–92.

4. **Langley J, Hall P and Newham P** (1993) Novel ultra wide-bandwidth Vivaldi antenna with low cross polarisation. *Electronics Letters* **29**, 2004–2005.

5. **Liu Y, Zhou W, Yang S, Li W, Li P and Yang S** (2016) A novel miniaturized Vivaldi antenna using tapered slot edge with resonant cavity structure for ultrawideband applications. *IEEE Antennas and Wireless Propagation Letters* **15**, 1881–1884.

6. **Wang Z, Yin Y, Wu J and Lian R** (2016) A miniaturized CPW-fed antipodal Vivaldi antenna with enhanced radiation performance for wideband applications. *IEEE Antennas and Wireless Propagation Letters* **15**, 16–19.

7. **Natarajan R, George JV, Kanagasabai M and Kumar Shrivastav A** (2015) A compact antipodal Vivaldi antenna for UWB applications. *IEEE Antennas and Wireless Propagation Letters* **14**, 1557–1560.

8. **Siddiqui JY, Antar YMM, Freundorfer AP, Smith EC, Morin GA and Thayaparan T** (2011) Design of an ultra wideband antipodal tapered slot antenna using elliptical strip conductors. *IEEE Antennas and Wireless Propagation Letters* **10**, 251–254.

9. **Zhang J, Liu S, Wang F, Yang Z and Shi X** (2017) A compact high-gain Vivaldi antenna with improved radiation characteristics. *Progress in Electromagnetics Research Letters* **68**, 127–133.

10. **Biswas B, Ghatak R and Poddar DR** (2017) A fern fractal leaf inspired wideband antipodal Vivaldi antenna for microwave imaging system. *IEEE Transactions on Antennas and Propagation* **65**, 6126–6129.

11. **Abbak M, Akınc MN, Çayören M and Akduman İ** (2017) Experimental microwave imaging with a novel corrugated Vivaldi antenna. *IEEE Transactions on Antennas and Propagation* **65**, 3302–3307.

12. **Moosazadeh M, Kharkovsky S, Case JT and Samali B** (2017) Miniaturized UWB antipodal Vivaldi antenna and its application for detection of void inside concrete specimens. *IEEE Antennas and Wireless Propagation Letters* **16**, 1317–1320.

13. **Zhang X, Chen Y, Tian M, Liu J and Liu H** (2018) A compact wideband antipodal Vivaldi antenna design. *International Journal of RF and Microwave Computer-Aided Engineering* **29**, 1–6.

14. **Yang K, Hoang M, Bao X, McEvoy P and Ammann MJ** (2018) Dual-stub Ka-band Vivaldi antenna with integrated bandpass filter. *IET Microwaves, Antennas & Propagation* **12**, 668–671.

15. **Yang D, Zeng H, Liu S and Pan J** (2016) A Vivaldi antenna with switchable and tunable band-notch characteristic. *Progress in Electromagnetics Research C* **68**, 75–83.

16. **Gao C, Li E, Zhang Y and Guo G** (2018) A directivity enhanced structure for the Vivaldi antenna using coupling patches. *Microwave and Optical Technology Letters* **60**, 418–424.

17. **Yin Z, Yang X-X, Yu F and Gao S** (2020) A novel miniaturized antipodal Vivaldi antenna with high gain. *Microwave and Optical Technology Letters* **62**, 418–424.

18. **Natarajan R, Gulam Nabi Alsath M, Kanagasabai M, Bilvam S and Meiyalagan S** (2020) Integrated Vivaldi antenna for UWB/diversity applications in vehicular environment. *International Journal of RF and Microwave Computer-Aided Engineering* **30**, 1–10.

19. **Meng X, Wu B, Huang Z and Wu X** (2016.) Compact 30:1 bandwidth ratio Balun for printed balanced antennas. *Progress in Electromagnetics Research C* **64**, 125–132.

20. **Dzagbletey PA, Shim J-Y and Chung J-Y** (2019) Quarter-wave balun fed Vivaldi antenna pair for V2X communication measurement. *IEEE Transactions on Antennas and Propagation* **67**, 1957.

21. **Lin S, Wang J, Deng Y and Zhang G.** (2015) A new compact ultra-wideband balun for printed balanced antennas. *Journal of Electromagnetic Waves and Applications* **29**, 1570–1579. doi: 10.1080/09205071.2015.1051191.

22. **Song L and Zhou H** (2018) Wideband dual-polarized Vivaldi antenna with improved balun feed. *International Journal of Microwave and Wireless Technologies* **11**(1), 1–12.

23. **Pandey GK, Verma H and Meshram MK** (2015) Compact antipodal Vivaldi antenna for UWB applications. *IEEE Antennas and Wireless Propagation Letters* **51**, 308–310.

24. **Yao Y, Cheng X, Wang C, Yu J and Chen X** (2017) Wideband circularly polarized antipodal curvedly tapered slot antenna array for 5G applications. *IEEE Journal on Selected Areas in Communications* **35**, 1539–1549.

25. **Bourqui J, Okoniewski M and Fear EC** (2010) Balanced antipodal Vivaldi antenna with dielectric director for near-field microwave imaging. *IEEE Transactions on Antennas and Propagation* **58**, 2318–2326.

26. **Wang P, Zhang H, Wen G and Sun Y** (2012) Design of modified balanced antipodal Vivaldi antenna. *Progress in Electromagnetics Research C* **25**, 271–285.

27. **Etesami F, Khorshidi S, Shahcheraghi S and Yahaghi A** (2017.) Improvement of radiation characteristics of balanced antipodal Vivaldi antenna using transformation optics. *Progress in Electromagnetics Research* **56**, 189–196.

28. **Li L, Xia X, Liu Y and Yang T** (2016) Wideband balanced antipodal Vivaldi antenna with enhanced radiation parameters. *Progress in Electromagnetics Research C* **66**, 163–171.

29. **Wang NN, Fang M, Chou HT, Qi JR and Xiao LY** (2018) Balanced antipodal Vivaldi antenna with asymmetric substrate cutout and dual scale slotted edges for ultrawideband operation at millimeter-wave frequencies. *IEEE Transactions on Antennas and Propagation* **66**, 3724–3729.

30. **Sarkar C, Saha C, Shaik LA, Siddiqui JY and Antar YMM** (2018) Frequency notched balanced antipodal tapered slot antenna with very low cross-polarised radiation. *IET Microwaves Antennas & Propagation Research* **12**, 1859–1863.

31. **Wang P, Wen G, Zhang H and Sun Y** (2013) A wideband conformal end-fire antenna array mounted on a large conducting cylinder. *IEEE Transactions on Antennas and Propagation* **61**, 4857–4861.

32. **Federal Communications Commission** (2002) Revision of Part 15 of the commission's rules regarding ultra-wideband transmission systems, FIRST REPORT AND ORDER. ET Docket 98–153, FCC 02-48, 1–118, Feb. 14, 2002.

33. **Bai J, Shi S and Prather DW** (2011) Modified compact antipodal Vivaldi antenna for 4–50-GHz UWB application. *IEEE Transactions on Microwave Theory and Techniques* **59**, 1501–1507.

34. **Moosazadeh M** (2018) High-gain antipodal Vivaldi antenna surrounded by dielectric for wideband applications. *IEEE Transactions on Antennas and Propagation* **66**, 4349–4352.

35. **Krishna GV, Madhav BTP, Giridhar MV, Reddiah Babu MV, Sai Krishna V and Mohan Reddy SS** (2013) Bandwidth enhanced antipodal Vivaldi antenna for wide band communication applications. *Indian Journal of Science and Technology* **9**, 1–6.

36. **Tianang EG, Elmansouri MA and Filipovic DS** (2018) Ultra-wideband lossless cavity-backed Vivaldi antenna. *IEEE Transactions on Antennas and Propagation* **66**, 115–124.

37. **Zhu S, Liu H, Chen Z and Wen P** (2018) A compact gain-enhanced Vivaldi antenna array with suppressed mutual coupling for 5 G mmwave application. *IEEE Antennas and Wireless Propagation Letters* **17**, 776–779.

38. **Elsheakh DM, Eltresy NA and Abdallah EA** (2017) Ultra wide bandwidth high gain Vivaldi antenna for wireless communications. *Progress in Electromagnetics Research Letters* **69**, 105–111.

39. **Elsheakh DM and Abdallah EA** (2014) Ultrawideband Vivaldi antenna for DVB-T, WLAN, and WiMAX applications. *International Journal of Antennas and Propagation* **2014**, 1–7.

40. **Hood AZ, Karacolak T and Topsakal E** (2008) A small antipodal Vivaldi antenna for ultrawide-band applications. *IEEE Antennas and Wireless Propagation Letters* **7**, 656–660.

41. **Mehdipour A, Mohammadpour-Aghdam K and Faraji-Dana R** (2007) Complete dispersion analysis of Vivaldi antenna for UWB applications. *Progress in Electromagnetics Research, PIER* **77**, 85–96.

42. **Kumar M and Nath V** (2018) Introducing multiband and wideband microstrip patch antennas using fractal geometries: development: in last decade. *Wireless Personal Communications* **98**, 2079–2105.

43. **de Oliveira AM, Justo JF, Perotoni MB, Kofuji ST, Neto AG, Bueno RC and Baudrand H** (2017) A high directive Koch fractal Vivaldi antenna design for medical near-field microwave imaging applications. *Microwave and Optical Technology Letters* **59**, 337–346.

44. **Karmakar A, Bhattacharjee A, Saha A and Bhawal A** (2019) Design of a fractal inspired antipodal Vivaldi antenna with enhanced radiation characteristics for wideband applications. *IET Microwaves, Antennas & Propagation* **13**, 892–897.

45. **Moosazadeh M, Kharkovsky S and Case JT** (2016) Microwave and millimetre wave antipodal Vivaldi antenna with trapezoid-shaped dielectric

lens for imaging of construction materials. *IET Microwaves, Antennas & Propagation* 10, 301–309.

46. **Moosazadeh M and Kharkovsky S** (2015) Development of the antipodal Vivaldi antenna for detection of cracks inside concrete members. *Microwave and Optical Technology Letters* 57, 1573–1580.

47. **Pandey GK, Singh HS, Bharti PK, Pandey A and Meshram MK** (2015) High gain Vivaldi antenna for radar and microwave imaging applications. *International Journal of Signal Processing Systems* 3, 35–40.

48. **Mahmud M, Islam M, Rahman M, Alam T and Samsuzzaman M** (2017) A miniaturized directional antenna for microwave breast imaging applications. *International Journal of Microwave and Wireless Technologies* 9, 2013–2018.

49. **Juan L, Guang F, Lin Y and Demin F** (2013) A modified balanced antipodal Vivaldi antenna with improved radiation characteristics. *Microwave and Optical Technology Letters* 55, 1321–1325.

50. **Moosazadeh M, Kharkovsky S, Esmati Z and Samali B** (2016) UWB elliptically-tapered antipodal Vivaldi antenna for microwave imaging applications. IEEE-APWC, pp. 102–105.

51. **Moosazadeh M, Kharkovsky S, Case JT and Samali B** (2017) Antipodal Vivaldi antenna with improved radiation characteristics for civil engineering applications. *IET Microwaves, Antennas & Propagation* 11, 796–803.

52. **Bah MH, Hong J, Jamro DA, Liang JJ and Kponou EA** (2014) Vivaldi antenna and breast phantom design for breast cancer imaging. International Conference on BioMedical Engineering and Informatics, pp. 90–93.

53. **Amiri M, Tofigh F, Ghafoorzadeh-Yazdi A and Abolhasan M** (2017) Exponential antipodal Vivaldi antenna with exponential dielectric lens. *IEEE Antennas and Wireless Propagation Letters* 16, 1792–1795.

54. **Moosazadeh M, Kharkovsky S, Case JT and Samali B** (2017) Improved radiation characteristics of small antipodal Vivaldi antenna for microwave and millimeter-wave imaging applications. *IEEE Antennas and Wireless Propagation Letters* 16, 1961–1964.

55. **Akhter Z, Abhijith BN and Akhtar MJ** (2016) Hemisphere lens-loaded Vivaldi antenna for time domain microwave imaging of concealed objects. *Journal of Electromagnetic Waves and applications* 30, 1183–1197.

56. **Wan F, Chen J and Li B** (2018) A novel ultra-wideband antipodal Vivaldi antenna with trapezoidal dielectric substrate. *Microwave and Optical Technology Letters* 60, 449–455.

57. **Moosazadeh M and Kharkovsky S** (2016) A compact high-gain and front-to-back ratio elliptically tapered antipodal Vivaldi antenna with trapezoid-shaped dielectric Lens. *IEEE Antennas and Wireless Propagation Letters* 15, 552–555.

58. **Teni G, Zhang N, Qiu J and Zhang P** (2013) Research on a novel miniaturized antipodal Vivaldi antenna with improved radiation. *IEEE Antennas and Wireless Propagation Letters* 12, 417–420.

59. **Kota K and Shafai L** (2011) Gain and radiation pattern enhancement of balanced antipodal Vivaldi antenna. *Electronics Letters* 47, 303–304.

60. **Zhang Y, Li E, Wang C and Guo G** (2017) Radiation enhanced Vivaldi antenna with double-antipodal structure. *IEEE Antennas and Wireless Propagation Letters* 16, 561–564.

61. **Li XX, Xu Y, Wang H, Zhang Y and Lv G** (2018) Low cross-polarization antipodal tapered slot antenna with gain, bandwidth enhancement for UWB application. *Journal of Computational Electronics* 17, 442–451.

62. **Li XX, Pang DW, Wang HL, Zhang YM and Lv GQ** (2017) Dielectric slabs covered broadband Vivaldi antenna for gain enhancement. *Progress in Electromagnetics Research C* 77, 69–80.

63. **Nassar IT and Weller TM** (2015) A novel method for improving antipodal Vivaldi antenna performance. *IEEE Transactions on Antennas and Propagation* 63, 3321–3324.

64. **Li Z, Kang X, Su J, Guo Q, Yang Y and Wang J** (2016) A wideband endfire conformal Vivaldi antenna array mounted on a dielectric cone. *International Journal of Antennas and Propagation* 2016, 1–11.

65. **Eichenberger J, Yetisir E and Ghalichechian N** (2019) High-gain antipodal Vivaldi antenna with pseudoelement and notched tapered slot operating at (2.5 to 57) GHz. *IEEE Transactions on Antennas and Propagation* 67, 4357–4366.

66. **Sang L, Li X, Chen T and Lv G** (2017.) Analysis and design of tapered slot antenna with high gain for ultra wideband based on optimisation of the metamaterial unit layout. *IET Microwaves, Antennas & Propagation* 11, 907–914.

67. **Bhaskar M, Johari E, Akhter Z and Akhtar MJ** (2016) Gain enhancement of the Vivaldi antenna with band notch characteristics using zero index material. *Microwave and Optical Technology Letters* 58, 233–239.

68. **Pandey GK, Singh HS and Meshram MK** (2016) Meander-line-based inhomogeneous anisotropic artificial material for gain enhancement of UWB Vivaldi antenna. *Applied Physics A: Materials Science and Processing* 122, 1–9.

69. **Sun M, Chen ZN and Qing X** (2013) Gain enhancement of 60-GHz antipodal tapered slot antenna using zero-index metamaterial. *IEEE Transactions on Antennas and Propagation* 61, 1741–1746.

70. **Li X, Zhou H, Gao Z, Wang H and Lv G** (2017) Metamaterial slabs covered UWB antipodal Vivaldi antenna. *IEEE Antennas and Wireless Propagation Letters* 16, 2943–2946.

71. **Xu Y, Wang J, Ge L, Wang X and Wu W** (2018) Design of a notched-band Vivaldi antenna with high selectivity. *IEEE Antennas and Wireless Propagation Letters* 17, 62–65.

72. **Natarajan R, Kanagasabai M and Gulam Nabi Alsath M** (2016) Dual mode antipodal Vivaldi antenna. *IET Microwaves, Antennas & Propagation* 10, 1643–1647.

73. **Wu J, Zhao Z, Nie Z and Liu Q** (2014) A printed UWB Vivaldi antenna using stepped connection structure between slotline and tapered patches. *IEEE Antennas and Wireless Propagation Letters* 13, 698–701.

74. **Fusco PLVF** (2011) Antipodal Vivaldi antenna with tuneable band rejection capability. *IET Microwaves, Antennas & Propagation* 5, 372–378.

Anindita Bhattacharjee belongs from Agartala, Tripura, India. She received her BE degree in Electronics and Communication Engineering from Tripura Institute of Technology, under Tripura University (Central University), Tripura, India in 2014. She received the M.Tech degree in Electronics and Communication Engineering, from Tripura University (Central University), Tripura, India in 2018. Her research interests include analysis and design of compact antennas for wideband applications, ultra-wideband (UWB) antennas, fractal antennas, Vivaldi antenna, MIMO antenna. She has published a number of peer-reviewed journal papers and conference articles.

Abhirup Bhawal belongs from Kolkata, West Bengal, India. He received his B.Tech degree in Electronics and Communication Engineering from Birbhum Institute of Engineering and Technology and M.Tech degree in Communication Engineering from Netaji Subhash Engineering College, under the West Bengal University of Technology, Kolkata, West Bengal, India in 2011 and 2014, respectively. He is currently pursuing the Ph.D. degree in the Department of Electronics and Communication Engineering, Tripura University (A Central University), Tripura, India. His research interests include analysis and design of compact antennas for wideband applications, ultra-wideband (UWB) antennas, fractal antennas, Vivaldi antennas as well as antennas having special applications like medical imaging, ground-penetrating RADAR, WiFi, etc. He has published several peer-reviewed journal papers and conference articles. He has worked as an Assistant Professor at the Electronics and Communication Engineering Department of Techno India, India.

Dr. Anirban Karmakar has completed his Ph.D. degree in Engineering from Jadavpur University, Kolkata, India, in 2015. He has more than 13 years of teaching experience and is currently holding the post of Assistant Professor in the Department of Electronics & Communication Engineering at Tripura University (A Central University), India. He has almost 40 research articles in refereed journals and international conference proceedings. He has served as a reviewer in different international journals. He was awarded the best paper award from different international

conferences. He is a Senior Member of IEEE and has organized different workshops in the capacity of a convener and completed various funded projects received from UGC. Currently, four research scholars are pursuing Ph.D. under his guidance. His areas of interest include planar and fractal wideband antennas, Arrays, Circular Polarized Antennas, DRA, etc.

Dr. Anuradha Saha received the gold medal for securing 1st rank in M.Tech. degree in Mechatronics from the National Institute of Technical Teachers' Training and Research, Kolkata in 2009 and obtained Ph.D. degree in Engineering from Jadavpur University in 2017. She has been working as an Assistant Professor in the Department of Applied Electronics and Instrumentation Engineering since 2008 in Netaji Subhash Engineering College, Kolkata, wherein between she has served as full-time research scholar from 2012 to 2015 at the Department of Electronics and Telecommunication Engineering of Jadavpur University, funded by UGC. She is the author of over 30 publications in top international journals and conference proceedings. Her research interests include Artificial Intelligence, Pattern Recognition, Cognitive Robotics, Human-Computer-Interaction as well as Antennas. She is the reviewer of some renowned journals including IEEE Transactions on Fuzzy Systems, IEEE Transactions on Emerging Topics in Computational Intelligence, IETE Journal of Research, and so on.

Dr. Diptendu Bhattacharya received the B.E. degree from the National Institute of Technology, Jaipur, Rajasthan, India and M.E.Tel.E. (Computer Engineering) from Jadavpur University, Kolkata, India, in 1988 and 1999 respectively. He is currently an Associate Professor in the Department of Computer Science and Engineering, National Institute of Technology, Agartala, Tripura, India. He completed Ph.D. (Engineering) as a QIP Ph.D. fellow from Jadavpur University, Kolkata in 2016. He is working on Machine Intelligence in Economic Time-series prediction. He shouldered administrative responsibilities like Head of Department of Computer Science and Engineering, in the National Institute of Technology, Agartala. He supervised several B.Tech and M.Tech thesis in his teaching period in NIT, Agartala. Presently he is supervising Ph.D. students in NIT Agartala. He is the author of the book "*Time Series Prediction and Business Forecasting: A Machine Intelligence Approach*" published by Springer, Intelligent Systems Reference Library. His current research interests include type-2 fuzzy sets, artificial intelligence, computational intelligence, fuzzy time-series and its prediction.